 FDMP, vol.2, no.1, pp.1-15, 2006

# Scaffolds and Fluid Flow in Cardiac Tissue Engineering

**Milica Radisic[1] Chris Cannizzaro[2] and Gordana Vunjak-Novakovic[3]**

**Abstract:** To engineer cardiac tissue *in vitro* with properties approaching those of native tissue, it is necessary to reproduce many of the conditions found *in vivo*. In particular, cell density must be sufficiently high to enable contractility, which implies a three-dimensional culture with a sufficient oxygen and nutrient supply. In this review, hydrogels and scaffolds that support high cell densities are examined followed by a discussion on the utility of scaffold perfusion to satisfy high oxygen demand of cardiomyocytes and an overview of new bioreactors developed in our laboratory to accomplish this task more simply.

## 1 Introduction:

Nearly 8 million people in the United States have suffered from myocardial infarction, with 800,000 new cases occurring each year (American Heart Association, 2004). Myocardial infarction results in massive cell death in the infarct zone followed by pathological remodelling of the heart. The remodelling process involves cardiac dilation, wall thinning and severe deterioration of contractile function leading to congestive heart failure in more than 500,000 patients in the U.S. each year (American Heart Association, 2002). Conventional therapies are limited by the very limited ability of myocardium to regenerate after injury (Soonpaa and Field, 1998) and the shortage of organs available for transplantation. Cell based therapies such as cell injection and tissue engineering have been considered as novel treatment options (Reinlib and Field, 2000). This review will focus on some of the recent advances in cardiac tissue engineering with focus on two distinct regulatory factors: biomaterial scaffolds use as structural templates for cell attachment and tissue formation, and fluid flow in bioreactors utilized to engineer cardiac tissue.

[1] Institute of Biomaterials and Biomedical Engineering and Department of Chemical Engineering and Applied Chemistry, University of Toronto. Havard-MIT Division of Health Science and Technology.

[2] Massachusetts Institute of Technology

[3] Correspondence author, Department of Biomedical Engineering, Columbia University, New York, NY 10027, Email: gv2131@columbia.edu

## 2 Scaffold based approaches

Small infarcts may be treated by cells alone, whereas larger areas of damaged tissue may require excision and replacement with a cardiac patch. The time post-infarction is critical in the success of any regeneration strategy. Upon myocardial infarction, a vigorous inflammatory response is elicited and dead cells are removed by marrow-derived macrophages. Over the subsequent period of time ranging from weeks to months, fibroblasts and endothelial cells proliferate and form granulation tissue that eventually transforms into a dense collagenous scar. Formation of scar tissue severely reduces contractile function of the myocardium and leads to thinning and dilation of the ventricle wall, further remodeling and ultimately to heart failure. The regeneration strategy thus depends on the time post-infarction, i.e. new and old infarcts most likely cannot be treated using the same approach.

Cell injection strategies, will work best if applied shortly after myocardial infraction (MI). Application of cells and growth factors within a short period of time (hours to days) after MI has a potential of directing the wound repair process so that the minimum amount of scar tissue is formed, the contractile function is maintained in the border zone, and pathological remodelling is attenuated. Tissue engineering strategies will likely work in the acute phase as well, but they are probably more necessary after scar has formed. Then larger areas of heart must be replaced or augmented and this is potentially where a scaffold based approach may be most useful.

### *2.1 Cell-free cardiac patches*

Patients with large transmural akinetic scars often benefit from the endoventricular circular patch plasty known as the Dor procedure (Di Donato et al., 1997; Dor et al., 1989). In this procedure the scar tissue is excised and the ventricle is closed using a circular Dacron (polyethy-

lene terephtalate) patch lined with endocardium. In some cases, however, the success of this procedure is temporary, thus motivating the need for viable tissue patches. Another strategy to address pathological remodelling and prevent heart failure is a CorCap cardiac support device, an implant-grade Dacron mesh, that is wrapped around the heart ventricle to prevent further dilatation and support contractile function. In clinical trials, it was demonstrated that it results in improved quality of life, as well as improved heart size and shape (Starling and Jessup, 2004).

### *2.2 Cell based cardiac patches*

Approaches explored toward engineering a cell-based, functional cardiac patch that could be used to repair heart muscle utilized cell self-assembly, cells grown in hydrogels, porous and fibrous scaffolds, cultivation of thin films (sheets) of functionally coupled cells, and cells grown on composite scaffolds.

### *2.3 Self-assembly*

In cardiac tissue engineering approaches, most studies suggest that some type of scaffold, ideally in form of an inductive 3D matrix, is necessary to support assembly of cardiac tissue *in vitro*. An important scaffold-free approach includes stacking of confluent monolayers of cardiomyocytes (Shimizu et al., 2002). Although cardiac patches obtained in this way generate high active pulling force, engineering patches that are more than 2-3 cell layer thick remain a problem. Most recently, 24 mm long and 100 $\mu$m thick contractile cardiac organoids were fabricated by self-organization of the cells (Baar et al., 2005). Cardiomyocytes were cultivated on a PDMS surface coated with laminin. As laminin degraded, the confluent monolayer detached from the periphery of the substrate, moving towards the center and wrapping around a string placed in the center of the plate until a cylindrical contractile organoid was formed.

The scaffold approaches can be divided into i) hydrogel approaches where cells are either encapsulated and cultivated *in vitro* or injected directly into MI without pre-culture and ii) porous and fibrous 3D scaffold approaches where scaffolds are seeded with cells and in most cases cultivated *in vitro* prior to the utilization as cardiac patches.

### *2.4 Hydrogels*

The most important example of hydrogel based cardiac tissue engineering includes the work of Eschenhagen and colleagues. Cardiomyocytes were cast in growth factor supplemented collagen gels and cultivated in the presence of cyclic mechanical stretch (Eschenhagen et al., 1997; Fink et al., 2000; Zimmermann et al., 2002a; Zimmermann et al., 2000; Zimmermann et al., 2002b). The main advantage of tissue constructs grown using this approach is that they generated higher active force compared to tissues grown on porous or fibrous 3D scaffolds. In addition, collagen and laminin are the main components of the myocardial extracellular matrix, thus they support cardiomyocyte attachment and elongation. However, the main challenge remains tailoring the shape and dimensions of such tissues. One interesting approach to address this issue is the use of extruded collagen type I tubes (Yost et al., 2004).

A technique that can potentially combine the advantages of hydrogels with ease in tailoring tissue shape and size is inkjet printing. Cardiac constructs based on feline cardiomyocytes were created by printing cells dispersed in alginate and using calcium as a cross-linking agent. This approach may be particularly useful for co-culture of various cell types (Tao et al., 2004) as it enables precise control over cell location in the tissue construct.

Hydrogels were utilized to provide structural stability and deliver cells for regeneration of infarcted myocardium without the preculture stage. Various cell types were injected into myocardium using a biomaterial that solidifies upon injection such as Matrigel (Kofidis et al., 2004), fibrin glue (Christman et al., 2004a; Christman et al., 2004b; Ryu et al., 2005) or self-assembled peptides (Davis et al., 2005). In general, the studies report prevention of ventricle dilatation and improvement of fractional shortening and angiogenesis. Kofidis et al (Kofidis et al., 2004), reported that injection of Matrigel or Matrigel and ES cells into infarcted rat hearts resulted in structural stabilization, prevented wall thinning and improved fractional shortening. Chirsman et al (Christman et al., 2004a; Christman et al., 2004b) demonstrated that injection of skeletal myoblasts into myocardial infarcts using fibrin glue increased cell localization within the infarct after five weeks, reduced infarct size and increased vasularization of the scar without causing significant inflammatory response or foreign body reaction. Similarly, Ryu Hee et al (Ryu et al., 2005) found that injection of

bone marrow mononuclear cells into cryoinjured rat myocardium using fibrin matrix increased the amount of viable tissue and microvessel formation and reduced the amount of fibrous tissue in comparison to the injection of cells suspended in culture medium or culture medium alone. Recently, it was demonstrated that a synthetic material, self-assembling peptide hydrogel, can also be utilized for cell injection into the myocardium (Davis et al., 2005). Upon injection, the peptide formed a nano-fibrous structure that promoted recruitment of endogenous cells expressing endothelial markers, and supported survival of injected cardiomyocytes.

### *2.5 Porous scaffolds*

Three dimensional cardiac tissue constructs were successfully cultivated in dishes using a variety of scaffolds amongst which collagen sponges were the most common. In the pioneering approach of Li and colleagues, fetal rat ventricular cardiac myocytes were expanded after isolation, inoculated into collagen sponges and cultivated in static dishes for up to 4 weeks (Li et al., 1999). The cells proliferated with time in culture and expressed multiple sarcomeres. Adult human ventricular cells were used in a similar system, although they exhibited no proliferation (Li et al., 2000). Fetal cardiac cells were also cultivated on porous alginate scaffolds in static 96-well plates. After 4 days in culture the cells formed spontaneously beating aggregates in the scaffold pores (Leor et al., 2000). Cell seeding densities of the order of $10^8$cells/cm$^3$ were achieved in the alginate scaffolds using centrifugal forces during seeding (Dar et al., 2002). Neonatal rat cardiomyocytes formed spontaneously contracting constructs when inoculated in collagen sponges within 36 hr after seeding (Kofidis et al., 2003) and maintained their activity for up to 12 weeks. The contractile force increased upon addition of $Ca^{2+}$ and epinephrine.

### *2.6 Fibrous scaffolds*

In a classical tissue engineering approach, fibrous polyglycolic acid (PGA) (**Figure 1A**) scaffolds were combined with neonatal rat cardiomyocytes and cultivated in spinner flasks and rotating vessels (Carrier et al., 1999). The scaffold had 97% void volume and consisted of non-woven PGA fibres, 14$\mu$m in diameter. An advantage of this material is that the FDA already approves its use for biodegradable sutures. Neonatal rat or embryonic chick ventricular myocytes were seeded onto (PGA) scaffolds in spinner flasks, by placing scaffolds into a well-mixed cell suspension (magnetic stirring, 50rpm) (Carrier et al., 1999).

Constructs were subsequently cultured either in mixed flasks or in rotating bioreactor vessels. Mixing in the spinner flasks (0, 50, or 90 rpm) had a significant effect on the construct metabolism and cellularity. Constructs cultivated in mixed flasks had significantly higher cellularity index and metabolic activity compared to the constructs cultivated in the static flasks. After 1 week of culture, constructs made using neonatal rat heart cells contained a peripheral tissue-like region (50-70$\mu$m thick) in which cells stained positive for tropomyosin and organized in multiple layers in a 3-D configuration (Bursac et al., 1999) (**Figure 1A,B**). Electrophysiological studies conducted using a linear array of extracellular electrodes showed that the peripheral layer of the constructs exhibited relatively homogeneous electrical properties and sustained macroscopically continuous impulse propagation on a centimeter-size scale (Bursac et al., 1999). Constructs based on the cardiomyocytes enriched by preplating exhibited lower excitation threshold (ET), higher conduction velocity, higher maximum capture rate (MCR), and higher maximum and average amplitude. Laminar flow conditions in rotating bioreactors further improved the PGA based constructs. The cells in the peripheral layer expressed tropomyosin and had spatial distribution of connexin 43 comparable to that in neonatal rat ventricles. The expression levels of cardiac proteins connexin-43, creatin kinase-MM and sarcomeric myosin heavy chain were lower in rotating bioreactors cultivated constructs compared to the neonatal rat ventricle but higher than in the spinner flask cultivated constructs (Papadaki et al., 2001). It is important to note that in both spinner flasks and rotating bioreactors the center of the constructs was mostly acellular due to the diffusional limitations of oxygen transport to the cells.

Recently, electrospun scaffolds (**Figure 1C**) have gained significant attention as they enable control over structure at sub-micron levels as well as control over mechanical properties, both of which are important for cell attachment and contractile function. Entcheva and colleagues (Zong et al., 2005) used electrospinning to fabricate oriented biodegradable non-woven poly(lactide) (PLA) scaffolds. Neonatal rat cardiomyocytes cultivated on oriented PLA matrices, had remarkably well developed contractile apparatus (**Figure 1D**) and exhibited electrical

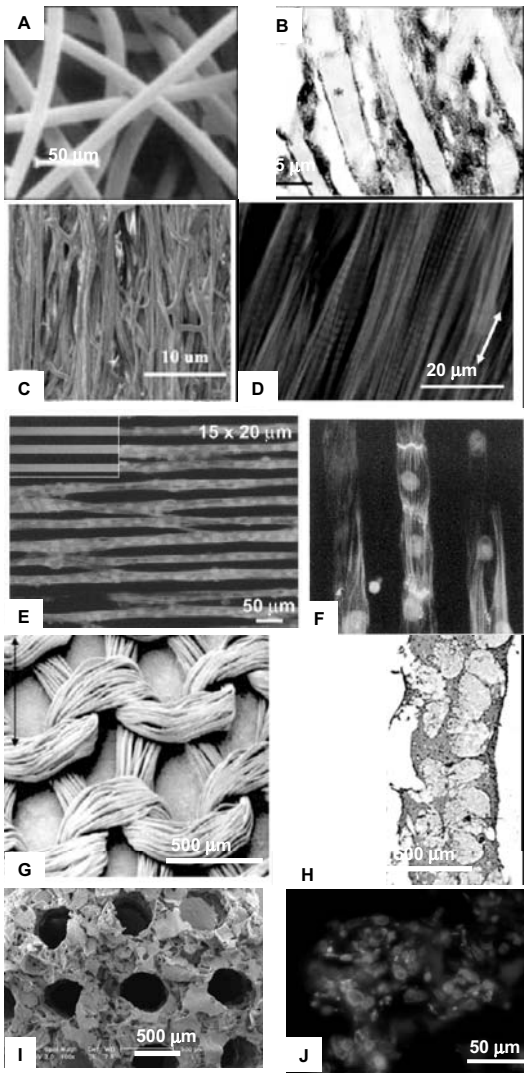


**Figure 1** : Representative scaffolds used in cardiac tissue engineering. A) Scanning electron micrograph of a non-woven fibrous PGA scaffold used in a classical approach by Freed and colleagues. B) Immunohistochemical staining for tropomyosin in constructs based on surface-hydrolyzed PGA seeded with neonatal rat cardiomyocytes and cultivated in rotating vessels for one week (reproduced with permission from (Papadaki et al., 2001) Figure 1B ). C) Scanning electron micrograph of a fibrous PLA scaffold obtained by electrospinning followed by uniaxial stretching (reproduced with permission from (Zong et al., 2005) Figure 1D) D) Neonatal rat cardyomyocytes cultured on oriented PLA scaffolds exhibited well developed contractile apparatus (actin-green) (reproduced with permission from (Zong et al., 2005) Figure 6C). E) Thin PLGA films patterned with laminin using microcontact printing (inset; 15$\mu$m laminin lanes spaced 20 $\mu$m apart) and seeded with neonatal rat cardiomyocytes (actin filaments-red, nuclei-blue) (reproduced with permission from (McDevitt et al., 2002) Figure 1A) F) Immunohistochemical staining illustrates elements of intercalated disks (N-cadherin-yellow, actin filaments-red). (reproduced with permission from (McDevitt et al., 2002) Figure 3) G) Scanning electron micrograph of the knitted Hylonect fabric; arrow indicates the direction cyclic stretch applied during culture (reproduced with permission from (Boublik et al., 2005) Figure 1A). (H) Cross-section of a construct sampled 2 h after cell seeding, showing the multifilament yarn (arrow) and immunohistochemical staining for cardiac troponin I. Neonatal rat cardiomyocytes were inoculated into the scaffold using fibrin (reproduced with permission from (Boublik et al., 2005) Figure 1B).

activity.

### 2.7 Thin films

A significant step forward toward engineering a clinically useful cardiac patch was the cultivation of cardiomyocytes derived from embryonic stem cells on thin polyurethane films. Cells exhibited cardiac markers (actinin) and were capable of synchronous macroscopic contractions (Alperin, Zandstra and Woodhouse, 2005). The orientation and cell phenotype could further be improved by microcontact printing of extracellular matrix components (e.g. laminin) as demonstrated for neonatal rat cardiomyocyte cultivated on thin polyurethane and PLA films (**Figure 1 E,F**) (McDevitt et al., 2002; McDevitt et al., 2003).

### 2.8 Combination approaches

To combine the benefits of the presence of naturally occurring extracellular matrix (laminin) and the structural stability of porous scaffolds, neonatal rat cardiomyocytes were inoculated into collagen sponges or synthetic polyglycerol sebacate scaffolds (PGS) using Matrigel (Radisic et al., in press). The main advantage of collagen sponges is that it supports cell attachment and differentiation. However, scaffolds tend to swell when placed in culture medium, and thus creation of a parallel channel array resembling a capillary network is difficult. For that purpose a novel biodegradable elastomer (Wang et al., 2002) with high degree of flexibility was used (**Figure 2 I**).

Freed and colleagues have recently reported that mechanical stimulation of hybrid cardiac grafts based on knitted hyaluronic acid based fabric and fibrin (Boublik et al., 2005) (**Figure 1G, H**). The grafts exhibited mechanical properties comparable to those of native neonatal rat hearts. In a subcutaneous rat implantation model the constructs exhibited the presence of cardiomyocytes and blood vessel ingrowth after 3 weeks.

## 3 Bioreactors and conditioning

Efforts in the development of bioreactors for tissue engineering of myocardium have focused on (a) providing sufficient oxygen supply for the highly metabolically active cardiomyocytes (Radisic et al., 2005a; Radisic et al., 2003; Radisic et al., 2004b) and (b) providing appropriate physical stimuli necessary to reproduce complex structure at various length scales (sub-cellular to tissue) (Radisic et al., 2004a; Zimmermann et al., 2002b). In this review we discuss medium perfusion as a tool to increase the thickness of the viable tissue. The methods to improve cell differentiation by physical stimulation (either mechanical stimulation or electrical) have been reviewed elsewhere.

Conventional culture vessels utilized for tissue engineering of the myocardium are static or mixed dishes, static or mixed flasks, and rotating bioreactors. These vessels offer three distinct flow conditions (static, turbulent, and laminar) and therefore differ significantly in the rate of oxygen supply to the surface of the tissue construct. Oxygen transport is a key factor for myocardial tissue engineering due to the high cell density and low tolerance of cardiac myocytes to hypoxia. In all configurations, oxygen is supplied only by diffusion from the surface to the interior of the tissue construct, yielding $\sim$100 $\mu$m thick surface layer of compact tissue capable of electrical signal propagation and an acelluar interior (Radisic et al., 2005b).

### 3.1 Interstitial medium flow

In order to increase the thickness of viable tissue, diffusional oxygen limitations have to be overcome during both cell seeding and tissue cultivation (**Figure 2A**). The technique of cell seeding that was specifically developed for cardiac tissue engineering involves (a) rapid inoculation of cardiac cells into collagen sponges using Matrigel®as a cell delivery vehicle, and (b) transfer of inoculated scaffolds into perfused cartridges with immediate establishment of the interstitial flow of culture medium through the seeded scaffolds. Forward-reverse flow was used for the initial period of 1.5 – 4.5 h in order to further increase the spatial uniformity of cell seeding (Radisic Biotech Bioeng. 2003). Unidirectional flow of culture medium was maintained for the duration of cultivation. In this system, cells were "locked" into the scaffold during a short (10 min) gelation period, and supplied with oxygen at all times during culture.

Constructs seeded in dishes had most cells located in the $\sim$100 $\mu$m thick layer at the top surface, and only a small number of cells penetrated the entire construct depth, while constructs seeded in perfusion had high and spatially uniform cell density throughout the perfused construct volume. Clearly, medium perfusion during seeding was key for engineering thick constructs with high densi-

ties of viable cells, presumably due to enhanced transport of oxygen within the construct.

Throughout the cultivation, the number of live cells in perfused constructs was significantly higher than in dish-grown constructs. Importantly, the final cell viability in perfused constructs (81.6 $\pm$ 3.7%) was not significantly different than the viability of the freshly isolated cells (83.8 $\pm$ 2.0) and it was markedly higher than the cell viability in dish-grown constructs (47.4 $\pm$ 7.8 %) (Radisic et al., 2004b). Consistently, the molar ratio of lactate produced to glucose consumed (L/G) was $\sim$ 1 for perfused constructs, indicating aerobic cell metabolism. In dishes, L/G increased progressively from 1 to $\sim$ 2, indicating a transition to anaerobic cell metabolism. Cell damage, assessed by monitoring the activity of lactate dehydrogenase (LDH) in culture medium, was at all time points significantly lower in perfusion than in dish cultures.

Perfused constructs and native ventricles had more cells in the S phase than in the G2/M phases, whereas the cells from dish-grown constructs appeared unable to complete the cell cycle and accumulated in the G2/M phase. Cells expressing cardiac-specific differentiation markers (sarcomeric $\alpha$-actin, sarcomeric tropomyosin, cardiac troponin I, **Figure 2A**) were present throughout the perfused constructs, and only within a $\sim$100 $\mu$m thick surface layer in dish-grown constricts. Spontaneous contractions were observed in some constructs early in culture, and ceased after approximately 5 days of cultivation, indicating the maturation of engineered tissue. In response to electrical stimulation, perfused constructs contracted synchronously, had lower excitation thresholds and recovered their baseline function levels following treatment with a gap junction blocker; dish-grown constructs exhibited arrhythmic contractile patterns and failed to recover their baseline levels.

Although interstitial medium flow enabled engineering of compact tissue that had physiologic density of viable aerobically metabolizing cells, most cells were round and mononucleated. This was likely due to the exposure of cardiac myocytes to hydrodynamic shear, in contrast to the native heart muscle where blood is confined within the capillary bed and therefore not in direct contact with cardiac myocytes. This motivated the design of scaffolds with arrays of channels that provide a separate compartment for medium flow.

### *3.2 Channelled scaffolds*

To test the feasibility of using channelled scaffolds, cardiac constructs were first engineered using a channelled collagen sponge (Ultrafoam$^{TM}$, 1 cm in diameter x 3 mm thick) seeded with neonatal cardiac myocytes and cultivated in perfusion at 0.5 ml/min for 10 days. The channel maintained its initial diameter and was surrounded with a 300 $\mu$m thick tissue layer. However, collagen is not optimal for cardiac tissue engineering due to its poor structural integrity. We thus explored the use of an elastomer, poly(glycerol sebacate), PGS (Wang et al., 2002), pretreated with cardiac fibroblasts and seeded with neonatal rat heart cells (**Figure 2B**). After 3 days of culture, cells on the scaffolds formed constructs that contracted synchronously in response to electrical stimulation. The scaffold pores remained open and the pressure drop measured across the construct was as low as 0.1 kPa/mm.

PGS is obtained by condensation of glycerol and sebacic acid, and formed by salt-leaching into a three-dimensional network with a desired pore size (e.g., $\sim$100 $\mu$m), porosity (95%), and thickness (1 - 5 mm). The cross-links and hydrogen bonds contribute to its unique elastic properties. PGS degrades by hydrolysis of its ester bond into glycerol (likely adsorbed in the body) and sebacic acid (secreted by urine either directly or metabolized into carboxylic acids). *In vivo* (5 weeks of subcutaneous implantation), PGS scaffold is biocompatible and biodegradable (linear loss of the scaffold mass to $\sim$20% of initial over 5 weeks of culture), such that its shape and structural integrity were well maintained. The mechanical properties of PGS resemble vulcanized rubber: PGS is highly elastic and capable of up to 400% elongation before it yields.

To mimic the capillary network, neonatal rat heart cells were cultured on PGS scaffolds with a parallel array of channels made using a laser cutting/engraving system (**Fig 2C**) and perfused with culture medium. To mimic oxygen supply by hemoglobin, culture medium was supplemented by 5.4 vol%v/v PFC emulsion (Oxygent$^{TM}$, kindly donated by Alliance Pharmaceuticals Corp. (San Diego CA); constructs perfused with unsupplemented culture medium served as controls. Constructs were subjected to unidirectional medium flow at a flow rate of 0.1 ml/min provided by a multi-channel peristaltic pump (IsmaTec, Switzerland) (**Figure 2B**).

As the medium flowed through the channel array, oxy-

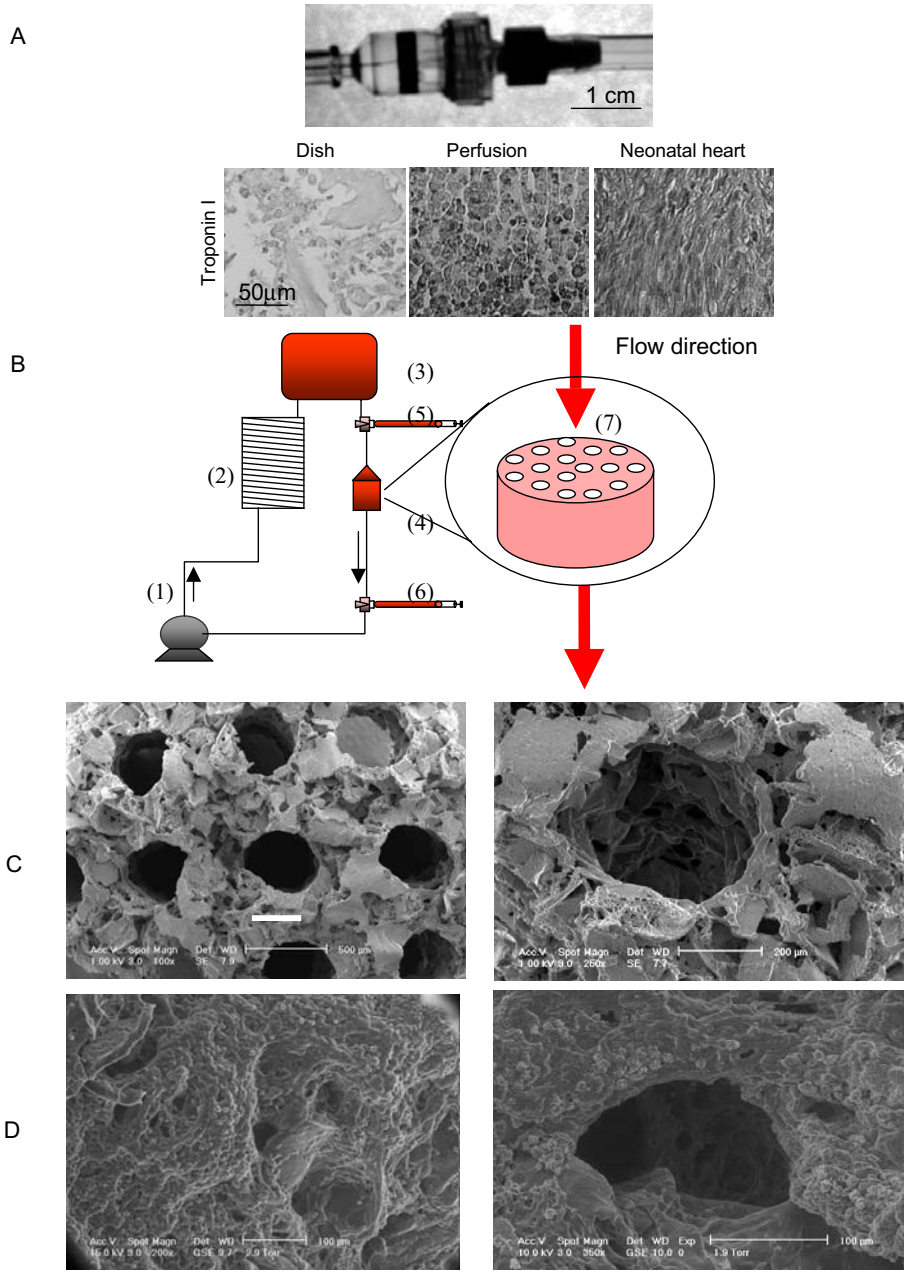


**Figure 2** : Cardiac tissue engineering culture systems focus on achieving adequate oxygen supply for highly metabolically active cells and providing appropriate physical cues that lead to differentiated phenotype **A** Direct culture medium perfusion of constructs based on neonatal rat cardiomyocytes inoculated into collagen sponges using Matrigel. Medium perfusion resulted in uniform cell distribution and maintenance of cell viability. Immunohistochemical staining illustrated corss-sectional distribution of cells expressing cardiac Troponin I. **B** Perfusion loop, consisting of channeled biorubber scaffolds (7), perfusion cartridges (4), two debubbling syringes (5, 6) a multi-channel peristaltic pump (1), a gas exchanger (2), and the reservoir bag (3) **C** Scanning electron micrograph of a parallel channel array bored in the PGS scaffolds using $CO_2$ laser/scanning engraving system. **D** Scanning electron micrograph of neonatal rat heart cells seeded onto channeled PGS scaffolds using Matrigel$^{TM}$ and cultivated in perfusion with 5.4 vol% perfluorocarbon emulsion supplemented culture medium. Scale bars: (C, left) 500 $\mu$m (C,right) 200 $\mu$m $\mu$m and (D) 100 $\mu$m.

gen was depleted from the aqueous phase of the culture medium by diffusion into the construct space where it was used for cell respiration. Depletion of oxygen in the aqueous phase acted as a driving force for the diffusion of dissolved oxygen from the PFC particles, thereby contributing to the maintenance of higher oxygen concentrations in the medium. Due to the small size of PFC particles, the passive diffusion of dissolved oxygen from the PFC phase into the aqueous phase was very fast, and estimated not to be a rate-limiting step in this system. For comparison, in un-supplemented culture medium, oxygen was depleted faster since there is no oxygen carrier phase that acts as a reservoir (Radisic et al., 2005a).

In PFC-supplemented medium, the decrease in the partial pressure of oxygen in the aqueous phase was only 50% of that in control medium (28 mmHg vs. 45 mmHg between the construct inlet and outlet at the flow rate of 0.1 ml/min). Consistently, constructs cultivated in the presence of PFC had higher amounts of DNA, troponin I and Cx-43, and significantly better contractile properties as compared to control constructs. In both groups, cells were present at the channel surfaces as well as within constructs. Improved constructs properties were correlated with the enhanced supply of oxygen to the cells within constructs (**Figure 2D**).

### *3.3 Theoretical considerations of oxygen transport in perfused cardiac constructs*

A steady state mathematical model was developed to describe the oxygen concentration profiles within the channels of the tissue construct (Radisic et al., 2005a) assuming local equilibrium between the PFC and aqueous phase at every point along the channel. It was demonstrated that the internal diffusion as well as the oxygen diffusion from the PFC droplet into the culture medium was not rate limiting. The main modes of oxygen transport in the channel lumen include convection in axial direction and diffusion in the radial direction:

$$[1+(K-1)\phi]\cdot v_z(r)\frac{\partial C_a}{\partial z} = D_{eff}\left[\frac{1}{r}\frac{\partial}{\partial r}\left(r\frac{\partial C_a}{\partial r}\right)+\frac{\partial^2 C_a}{\partial z^2}\right] \quad (1)$$

where K is partition coefficient, Vz ( r ) is velocity profile, $\phi$ is the volume fraction of PFC, Ca is oxygen concentration in the aqueos phase, and $D_{eff}$is effective diffusivity defined as:

$$D_{eff} = D_a\left(1+3\left(\frac{\gamma-1}{\gamma+2}\right)\phi\right) \quad (2)$$

where, $D_a$ is the diffusivity of $O_2$ in the aqueous phase, Dp is the diffusivity of $O_2$ in the PFC phase, $\gamma = KD_p/D_a$. Combining these equations yields the following conservation equation for the oxygen in the channel lumen:

$$[1+(K-1)\phi]\cdot v_z(r)\frac{\partial C_a}{\partial z} = D_{eff}\left[\frac{1}{r}\frac{\partial}{\partial r}\left(r\frac{\partial C_a}{\partial r}\right)+\frac{\partial^2 C_a}{\partial z^2}\right] \quad (3)$$

The simplified governing equation for oxygen distribution in the tissue space, where oxygen consumption is assumed to follow Michaelis-Menten kinetics is:

$$0 = D_t\left[\frac{1}{r}\frac{\partial}{\partial r}\left(r\frac{\partial C_t}{\partial r}\right)+\frac{\partial^2 C_t}{\partial z^2}\right]-\frac{V_{\max}C_t}{K_m+C_t} \quad (4)$$

where $C_t$is the oxygen concentration in the tissue space, Dt is diffusion coefficient in the tissue space, Vmax and Km are Michealis-Mentent parameters. For the measured inlet and outlet oxygen concentration, the following boundary conditions were used:

$$C_a(r,0) = C_{in} \quad (5)$$

$$C_t(r,0) = C_{in} \quad (6)$$

$$C_a(r,L) = C_{out} \quad (7)$$

$$C_t(r,L) = C_{out} \quad (8)$$

For predictions of oxygen concentration profiles at conditions that were not obtained experimentally, the inlet and outlet oxygen concentration were not measured. Therefore, an alternative set of boundary conditions was used. It was assumed that the culture medium entering the perfusion cartridge was fully saturated with oxygen and $C_a(r,0) = C_t$ (r,0) = 222.5 $\mu$M. The axial variations in the oxygen concentration cease to exist at the very short distance from the outlet of the channel array. Therefore,

$$\partial C_a/\partial z(r,L) = 0 \quad (9)$$

in the culture medium at the channel outlet. It was also assumed that the culture medium at the outlet was well

mixed, with no variations in the radial direction. Therefore, mixing cup concentration of the culture medium at the channel outlet was set to be boundary condition for the concentration at the tissue space outlet.

$$C_t(r,L) = \frac{\int_0^{R_c} C_a(r,L) v_z r dr}{\int_0^{R_c} v_z r dr} \quad (10)$$

The validity of the boundary conditions used for predictions was confirmed by comparing the oxygen concentration measured at the outlet of the experimentally obtained channeled tissue to the outlet values obtained using the described boundary conditions in the channel array of identical geometry, cell density and flow conditions.

Symmetry boundary condition was applied at the centerline of the channel lumen:

$$\partial C_a / \partial r(0,z) = 0 \quad (11)$$

The region supplied by each channel was approximated by a cylinder. Since these cylindrical regions are equally spaced a no flux boundary condition is applied at the half distance between channel centers ($R_t$), which is a common assumption in the well-known Krogh cylinder model.

$$\partial C_t / \partial r(R_t,z) = 0 \quad (12)$$

Finally, the fluxes of oxygen and the concentrations have to match at the interface between channel lumen and tissue space yielding the remaining two boundary conditions:

$$D_a \frac{\partial C_a}{\partial r}(R_c,z) = D_t \frac{\partial C_t}{\partial r}(R_c,z) \quad (13)$$

$$C_a(R_c,z) = C_t(R_c,z) \quad (14)$$

The model was solved for various channel geometries, flow rates and PFC emulsion volume fractions using the finite element method and commercial software Femlab. The results were expressed in terms of oxygen concentration in the aqueous phase [$\mu$M].

Experimentally obtained parameters were initially investigated and oxygen concentration profiles were generated for this system. The parameters included a channel diameter of 330 $\mu$m and a wall-to-wall spacing of 370 $\mu$m, perfused at an average linear velocity of 0.049 cm/s (0.1 mL/min bulk flow) and at 5.4 vol% of PFC emulsion. The Vmax was set to 10.5g$\mu$M/s (for PFC supplemented) and 8.8 $\mu$M/s (for pure culture medium) according to the measured protein content and reported maximum oxygen consumption per cell 27.6nmol/mg protein/min (Yamada et al., 1985) Aqueous phase oxygen concentrations at the inlet were comparable in the PFC-supplemented and control constructs in the channel lumen, but were lower in the tissue space in the PFC constructs, consistent with the higher cell densities in these constructs. However, moving along the length of the construct, the oxygen concentration in the lumen and tissue space of the PFC-supplemented construct was observed to be higher in comparison to the control construct, demonstrating the benefit of PFC supplementation. The differences in oxygen concentration in the tissue space were only evident at small depths, however, and became negligible at larger depths (Radisic et al., 2005a).

When the PFC concentration was varied (0, 3.2% and 6.4% v/v PFC) while maintaining the geometry and flow rate (0.049 cm/s), an overall increase in the oxygen concentration was observed with increasing PFC concentration in both the lumen and tissue space for both cell densities. However, even at the highest PFC concentration, 100 $\mu$m away from the lumen, the oxygen concentration dropped several orders of magnitude for physiological cell concentration of $10^8$ cells/cm$^3$ in the tissue space.

To address this issue, the geometry was optimized to a more closely packed one with a 100 $\mu$m channel diameter and 100 $\mu$m wall-to-wall spacing. As shown in **Figure 3A,** the oxygen concentration profile improved significantly when the fraction of PFC was increased from 0% to 6.4% v/v, but it was also necessary to increase the flow velocity from 0.049 cm/s to 0.135 cm/s to ensure all parts of the tissue space were being supplied adequately with oxygen. These flow rates had correspondingly normal wall shear stress values ($\sim$1 dyne/cm$^2$) that did not exceed values known to lead to decreased cell viability (Kretzmer and Schugerl, 1991; Stathopoulos and Hellums, 1985). Both the "coarse" and the "fine" geometry were fully compatible with the transport properties of blood (Radisic and Vunjak-Novakovic, 2005).

Analysis of the modeling parameters revealed that effective diffusivity of the medium was improved in the presence of PFC by up to 18% at the highest PFC fraction. Also, convective transport was increased up to 123%.

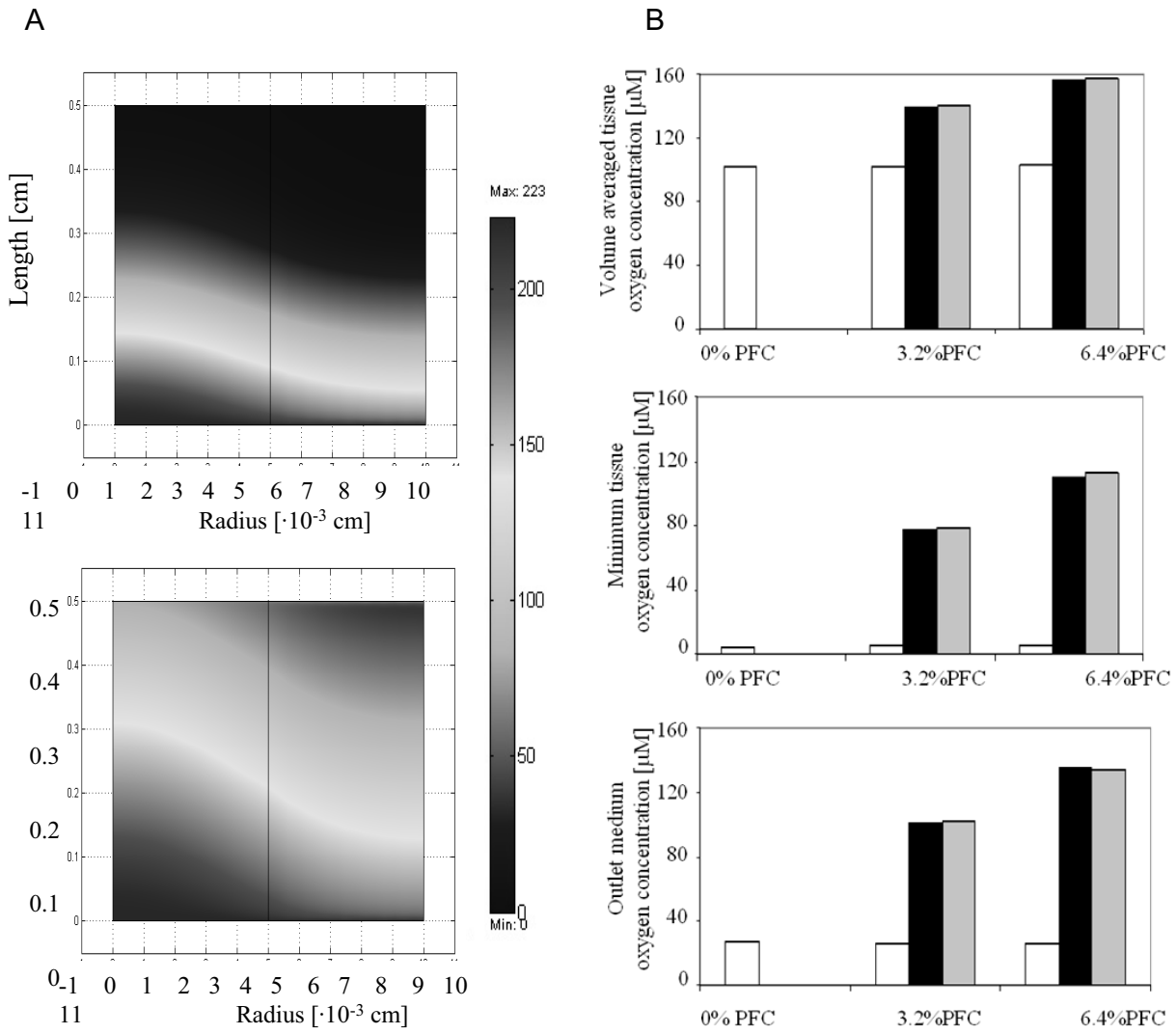


**Figure 3** : A) Oxygen concentration profile in the channel array. A 100 $\mu$m channel diameter and 100 $\mu$m wall-to-wall spacing was investigated in the model as an optimization to the in vitro parameters. The flow velocity was also increased in the range of 0.049 cm/s to 0.135 cm/s. A remarkable improvement in oxygen concentration is seen between (A) 0% PFC and (B) 6.4% PFC conditions. B) Overall effect of PFC emulsion on oxygen concentration in the cardiac constructs. Volume average oxygen concentration, minimum oxygen concentration, and mixing cup outlet concentration of oxygen in medium are shown as functions of PFC fraction (0, 3.2%, 6.4%). The contribution of PFC to the effective diffusivity (white bars) is compared to the contribution of PFC to the convective transport term (black bars), and the combination of both (grey bars). As shown, the effect of the PFC is dominated by its contribution to convective transport of oxygen.

This was validated by looking at the contributions of the diffusive and convective contributions of PFC supplementation, alone and in combination, on volume averaged tissue oxygen concentration, minimum tissue oxygen concentration, and mixing cup culture medium oxygen concentration at the outlet for zero order oxygen consumption kinetics (18 $\mu$M/s). As shown in **Figure 3B**, a significant increase is seen in all three parameters with increasing PFC concentration. More strikingly, the majority of the effect is due to the convective contribution of the PFC supplementation, with only a slight contribution from diffusion.

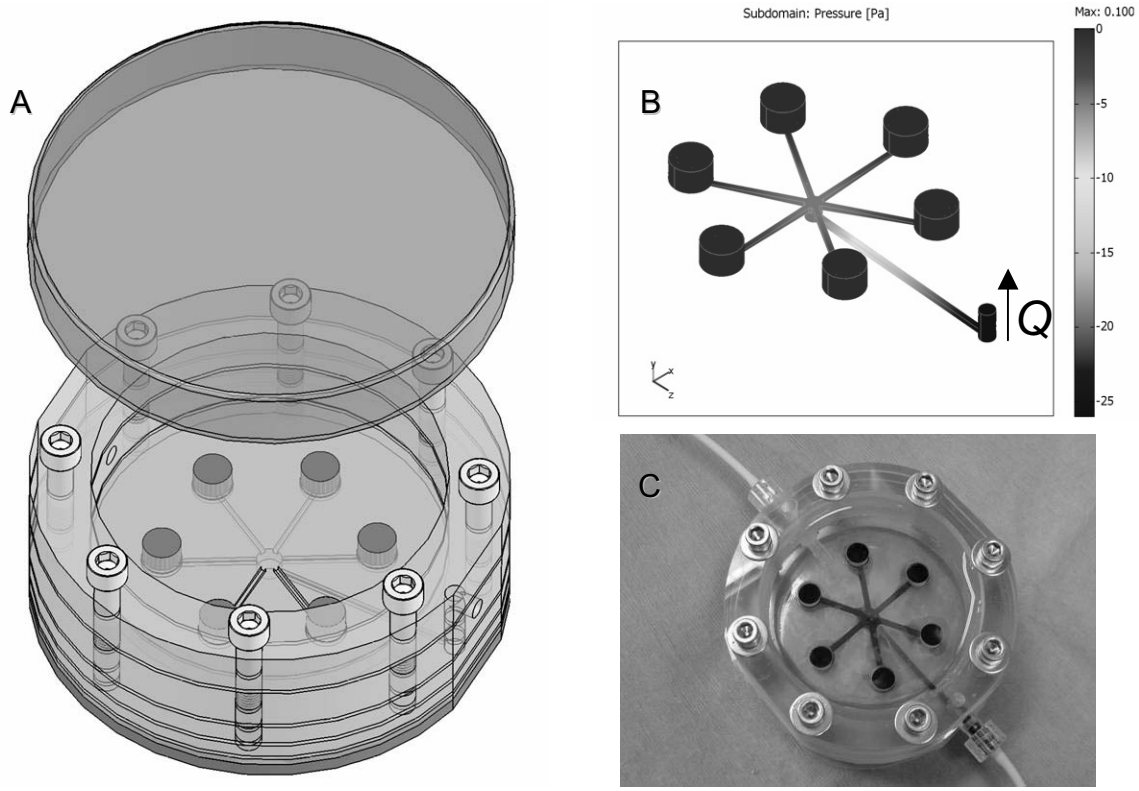


**Figure 4** : Perfusion bioreactor for six press-fit scaffolds. A. CAD model of perfusion bioreactor for six press-fit scaffolds; B. Cross-section view; C. Complete experimental setup showing perfusion loop and peristaltic pump.

### *3.4 Compatibility with flow properties of blood*

For *in vivo* implantation, it is essential that the geometry of the channelled cardiac constructs is compatible with the transport properties of blood. A physiological drop in the partial pressure of oxygen across tissues is from 95 mmHg in the arterial blood to 40 mmHg in venous blood (Fournier, 1998, p. 91). If the patch is grafted as an AV shunt, such that it connects to arterial blood at the inlet and venous blood at the outlet, the physiological difference in total oxygen concentration at the inlet and outlet will be 8630 - 5874 = 2756 ($\mu$M). Assuming that the patch has a physiologic density of cells metabolizing at Vmax, the metabolic demand for oxygen for the whole patch is 33$\mu$M/s. The calculated blood perfusion rate necessary to keep the cells well oxygenated under these conditions is 0.63 ml blood/cm$^3$ tissue/min, a value comparable to the reported baseline flow rates of blood in the heart (0.7 blood/cm$^3$ tissue/min, (Fournier, 1998, p. 95)).

For an engineered construct that is 0.5 cm in diameter and 0.5 cm thick, and contains an array of channels that are 100 $\mu$m in diameter and spaced at 100 $\mu$m apart, the model predicts a volumetric flow rate of blood of 1.9 $10^{-6}$ml/s per channel. The wall shear stress in the channels of the tissue graft perfused with blood can be estimated from the reduced average velocity ($4Q/\pi\ (2R_c)^3$) of the Casson fluid (Fournier, 1998, Eq. 3.21 ). The obtained wall shear stress of 0.99 dyn/cm$^2$ is high enough to avoid anomalous flow properties of blood that may occur at very low shear stresses, below the shear stress causing cell damage (1.6 dyn/cm$^2$) and sufficient to prevent spreading of leukocytes and pseudopode formation that may increase flow resistance at low shear rates and mediate inflammatory response (Moazzam et al., 1997). Also, the reduced average velocity of blood flow in the channels (2.5 s$^{-1}$) is greater than 1 s$^{-1}$, indicating that aggregation of red blood cells should not be expected. Finally, the pressure drop across the construct under these conditions (0.14 mm Hg) is considerably lower than that in the capillary bed (17 mmHg, (Fournier, 1998, p. 71)), and the total required blood flow was only 0.05 ml/min, indicating that the graft would not significantly increase the

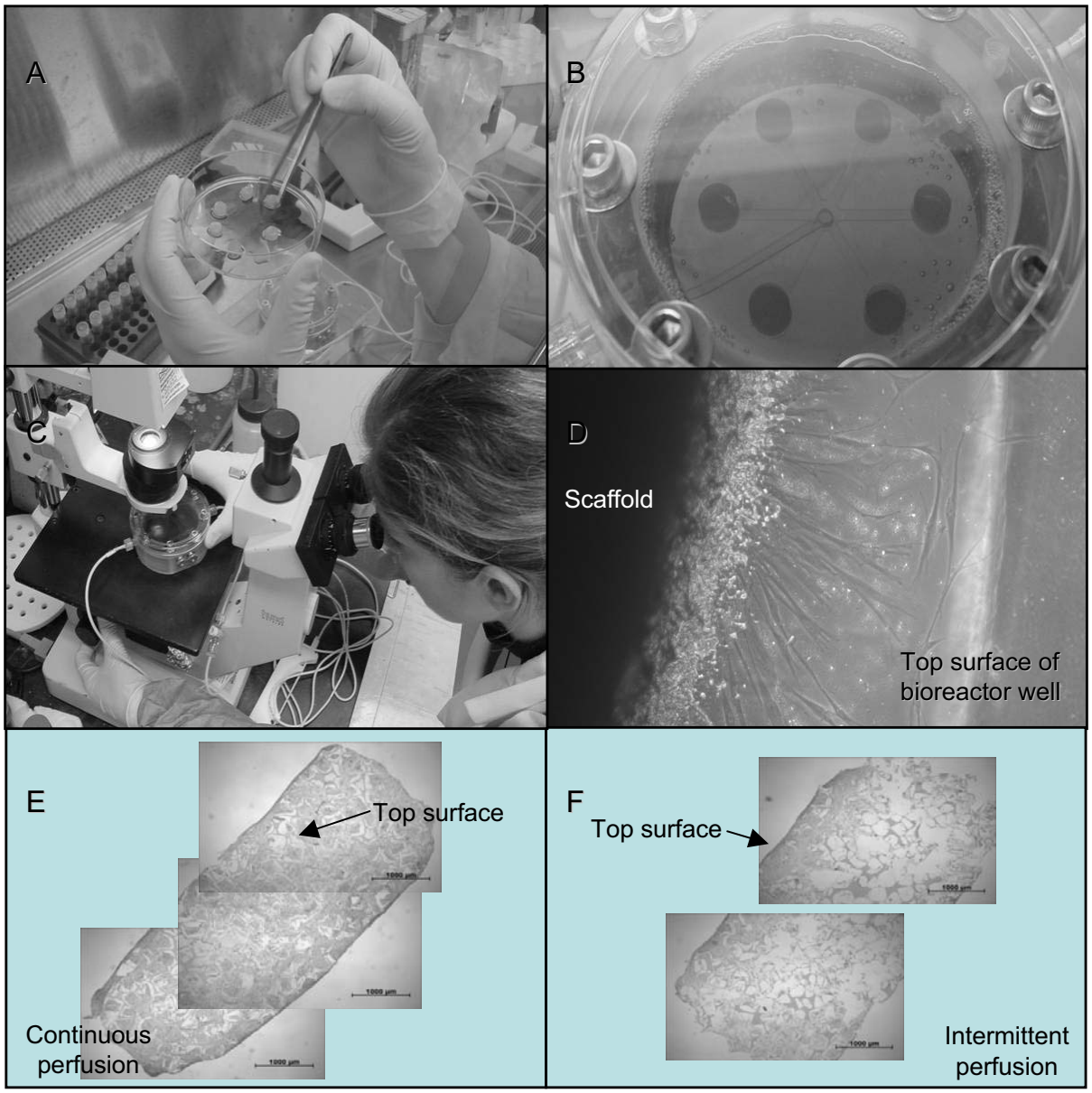


**Figure 5** : Engineering of perfused tissue. A. Scaffolds seeded with Mesenchymal stem cells; B. Perfusion bioreactor with seeded scaffolds; C. In situ imaging of scaffolds; D. Cell growth at scaffold periphery. E. Continuous scaffold perfusion (0.01 cm/s). F. Intermittent scaffold perfusion (0.01 cm/s for 1 h/day).

peripheral resistance for blood flow.

### *3.5 New bioreactors for scaffold perfusion*

Our initial system for scaffold perfusion (**Figure 2B**) demonstrated the importance of mass transport in engineering tissue with cell densities approaching that of native tissue. While effective, this system had several drawbacks: complicated setup with only one scaffold per perfusion loop, bubble entrapment, no imaging capability, etc. Our laboratory has since developed several bioreactors to address these concerns. One such design arranges the scaffolds in a radial pattern in what is essentially a functionalized Petri dish (**Figure 4A**). The bioreactor has the same dimensions as glass Petri dish, and makes use of a removable Petri dish cover that allows easy access to the scaffolds (**Figure 4B**). The bioreactor holds up to 40 ml of medium or approximately 7 ml of medium per scaffold. In addition to serving as a medium reservoir,

the space above the scaffolds serves as a gas exchanger and bubble trap. Below each scaffold, channels direct medium to a central hole, then down to a channel on the reverse surface, and finally to an external Luer fitting. A single perfusion loop transports medium to a peristaltic pump and then back to the bioreactor (**Figure 4C**). Finite element modeling (FEMLAB) was used to design a channel network with uniform velocity streamlines and a distributed pressure drop across all six scaffolds (**Figures 5A,B**),

Sequential images from a typical experiment are shown in **Figure 5**. The scaffolds were seeded external to the bioreactor and the cells were allowed to attach for several hours (**Figure 5A**). The scaffolds were then press-fit into individual wells and medium added (**Figure 5B**). The bioreactors were subsequently transferred to the incubator and perfusion started. Due to its low-profile design, scaffolds can be directly observed in situ (**Figure 5C**). Without staining, imaging within the scaffold was somewhat limited, though phase contrast alone was more than adequate to follow cell proliferation at scaffold edge (**Figure 5D**). Scaffolds continuously perfused at 0.01 cm/s over a three-week period exhibited a relatively homogeneous distribution of cells (**Figure 5E**), while in the case of intermittent perfusion cells were largely confined to the top layer of the scaffold (**Figure 5F**).

## References

**Alperin, C., Zandstra, P. W., and Woodhouse, K. A.** (2005): Polyurethane films seeded with embryonic stem cell-derived cardiomyocytes for use in cardiac tissue engineering applications. *Biomaterials*, vol. 26, no. 35, pp. 7377-7386.

**American Heart Association** (2002): Congestive heart failure.

**American Heart Association** (2004): Heart disease and stroke statistics-2004 update.

**Baar, K., Birla, R., Boluyt, M. O., Borschel, G. H., Arruda, E. M., and Dennis, R. G.** (2005): Self-organization of rat cardiac cells into contractile 3-d cardiac tissue. *Faseb J*, vol. 19, no. 2, pp. 275-277.

**Balsam, L. B., Wagers, A. J., Christensen, J. L., Kofidis, T., Weissman, I. L., and Robbins, R. C.** (2004): Haematopoietic stem cells adopt mature haematopoietic fates in ischaemic myocardium. *Nature*, vol. 428, no. 6983, pp. 668-673.

**Boublik, J., Park, H., Radisic, M., Tognana, E., Chen, F., Pei, M., Vunjak-Novakovic, G., and Freed, L. E.** (2005): Mechanical properties and remodeling of hybrid cardiac constructs made from heart cells, fibrin, and biodegradable, elastomeric knitted fabric. *Tissue Eng*, vol. 11, no. 7-8, pp. 1122-1132.

**Bursac, N., Papadaki, M., Cohen, R. J., Schoen, F. J., Eisenberg, S. R., Carrier, R., Vunjak-Novakovic, G., and Freed, L. E.** (1999): Cardiac muscle tissue engineering: Toward an in vitro model for electrophysiological studies. *American Journal of Physiology: Heart and Circulatory Physiology*, vol. 277, no. 46, pp. H433-H444.

**Carrier, R. L., Papadaki, M., Rupnick, M., Schoen, F. J., Bursac, N., Langer, R., Freed, L. E., and Vunjak-Novakovic, G.** (1999): Cardiac tissue engineering: Cell seeding, cultivation parameters and tissue construct characterization. *Biotechnology and Bioengineering*, vol. 64, pp. 580-589.

**Christman, K. L., Fok, H. H., Sievers, R. E., Fang, Q., and Lee, R. J.** (2004a): Fibrin glue alone and skeletal myoblasts in a fibrin scaffold preserve cardiac function after myocardial infarction. *Tissue Eng*, vol. 10, no. 3-4, pp. 403-409.

**Christman, K. L., Vardanian, A. J., Fang, Q., Sievers, R. E., Fok, H. H., and Lee, R. J.** (2004b): Injectable fibrin scaffold improves cell transplant survival, reduces infarct expansion, and induces neovasculature formation in ischemic myocardium. *J Am Coll Cardiol*, vol. 44, no. 3, pp. 654-660.

**Dar, A., Shachar, M., Leor, J., and Cohen, S.** (2002): Cardiac tissue engineering optimization of cardiac cell seeding and distribution in 3d porous alginate scaffolds. *Biotechnology and Bioengineering*, vol. 80, no. 3, pp. 305-312.

**Davis, M. E., Motion, J. P., Narmoneva, D. A., Takahashi, T., Hakuno, D., Kamm, R. D., Zhang, S., and Lee, R. T.** (2005): Injectable self-assembling peptide nanofibers create intramyocardial microenvironments for endothelial cells. *Circulation*, vol. 111, no. 4, pp. 442-450.

**Di Donato, M., Sabatier, M., Dor, V., Toso, A., Maioli, M., and Fantini, F.** (1997): Akinetic versus dyskinetic postinfarction scar: Relation to surgical outcome in patients undergoing endoventricular circular patch plasty repair. *J Am Coll Cardiol*, vol. 29, no. 7, pp. 1569-1575.

**Dor, V., Saab, M., Coste, P., Kornaszewska, M., and Montiglio, F.** (1989): Left ventricular aneurysm: A new surgical approach. *Thorac Cardiovasc Surg*, vol. 37, no. 1, pp. 11-19.

**Eschenhagen, T., Fink, C., Remmers, U., Scholz, H., Wattchow, J., Woil, J., Zimmermann, W., Dohmen, H. H., Schafer, H., Bishopric, N., Wakatsuki, T., and Elson, E.** (1997): Three-dimensional reconstitution of embryonic cardiomyocytes in a collagen matrix: A new heart model system. *FASEB Journal*, vol. 11, pp. 683-694.

**Fink, C., Ergun, S., Kralisch, D., Remmers, U., Weil, J., and Eschenhagen, T.** (2000): Chronic stretch of engineered heart tissue induces hypertrophy and functional improvement. *FASEB Journal*, vol. 14, pp. 669-679.

**Fournier, R. L.** (1998): Basic transport phenomena in biomedical engineering, Taylor & Francis, Philadelphia.

**Kofidis, T., Akhyari, P., Wachsmann, B., Mueller-Stahl, K., Boublik, J., Ruhparwar, A., Mertsching, H., Balsam, L., Robbins, R., and Haverich, A.** (2003): Clinically established hemostatic scaffold (tissue fleece) as biomatrix in tissue- and organ-engineering research. *Tissue Engineering*, vol. 9, no. 3, pp. 517-523.

**Kofidis, T., et al.** (2004): Injectable bioartificial myocardial tissue for large-scale intramural cell transfer and functional recovery of injured heart muscle. *Thorac Cardiovasc Surg*, vol. 128, pp. 571-5578.

**Kretzmer, G., and Schugerl, K.** (1991): Response of mammalian cells to shear stress. *Applied Microbiology and Biotechnology*, vol. 34, no. 5, pp. 613-616.

**Leor, J., Aboulafia-Etzion, S., Dar, A., Shapiro, L., Barbash, I. M., Battler, A., Granot, Y., and Cohen, S.** (2000): Bioengineerred cardiac grafts: A new approach to repair the infarcted myocardium? *Circulation*, vol. 102, no. suppl III, pp. III56-III61.

**Li, R.-K., Jia, Z. Q., Weisel, R. D., Mickle, D. A. G., Choi, A., and Yau, T. M.** (1999): Survival and function of bioengineered cardiac grafts. *Circulation*, vol. 100, no. Suppl II, pp. II63-II69.

**Li, R. K., Yau, T. M., Weisel, R. D., Mickle, D. A., Sakai, T., Choi, A., and Jia, Z. Q.** (2000): Construction of a bioengineered cardiac graft. *J Thorac Cardiovasc Surg*, vol. 119, no. 2, pp. 368-375.

**McDevitt, T. C., Angello, J. C., Whitney, M. L., Reinecke, H., Hauschka, S. D., Murry, C. E., and Stayton, P. S.** (2002): In vitro generation of differentiated cardiac myofibers on micropatterned laminin surfaces. *J Biomed Mater Res*, vol. 60, no. 3, pp. 472-479.

**McDevitt, T. C., Woodhouse, K. A., Hauschka, S. D., Murry, C. E., and Stayton, P. S.** (2003): Spatially organized layers of cardiomyocytes on biodegradable polyurethane films for myocardial repair. *J Biomed Mater Res A*, vol. 66, no. 3, pp. 586-595.

**Moazzam, F., DeLano, F. A., Zweifach, B. W., and Schmid-Schonbein, G. W.** (1997): The leukocyte response to fluid stress. *Proceedings of National Academy of Scince U S A*, vol. 94, no. 10, pp. 5338-5343.

**Papadaki, M., Bursac, N., Langer, R., Merok, J., Vunjak-Novakovic, G., and Freed, L. E.** (2001): Tissue engineering of functional cardiac muscle: Molecular, structural and electrophysiological studies. *American Journal of Physiology: Heart and Circulatory Physiology*, vol. 280, no. Heart Circ. Physiol. 44, pp. H168-H178.

**Radisic, M., Deen, W., Langer, R., and Vunjak-Novakovic, G.** (2005a): Mathematical model of oxygen distribution in engineered cardiac tissue with parallel channel array perfused with culture medium containing oxygen carriers. *American Journal of Physiology-Heart and Circulatory Physiology*, vol. 288, no. 3, pp. H1278-H1289.

**Radisic, M., Euloth, M., Yang, L., Langer, R., Freed, L. E., and Vunjak-Novakovic, G.** (2003): High density seeding of myocyte cells for tissue engineering. *Biotechnology and Bioengineering*, vol. 82, no. 4, pp. 403-414.

**Radisic, M., Malda, J., Epping, E., Geng, W., Langer, R., and Vunjak-Novakovic, G.** (2005b): Oxygen gradients correlate with cell density and cell viability in engineered cardiac tissue. *Biotechnol Bioeng*.

**Radisic, M., Park, H., Chen, F., Salazar-Lazzaro, J. E., Wang, Y., Dennis, R. G., Langer, R., Freed, L. E., and Vunjak-Novakovic, G.** (in press): Biomimetic approach to cardiac tissue engineering: Oxygen carriers and channeled scaffolds. *Tissue Eng*.

**Radisic, M., Park, H., Shing, H., Consi, T., Schoen, F. J., Langer, R., Freed, L. E., and Vunjak-Novakovic, G.** (2004a): Functional assembly of engineered myocardium by electrical stimulation of cardiac myocytes cultured on scaffolds. *Proceedings of the National Academy of Sciences of the United States of America*, vol. 101, no. 52, pp. 18129-18134.

**Radisic, M., and Vunjak-Novakovic, G.** (2005): Cardiac tissue engineering. *Journal of the Serbian Chemical Society*, vol. 70, no. 3, pp. 541-556.

**Radisic, M., Yang, L., Boublik, J., Cohen, R. J., Langer, R., Freed, L. E., and Vunjak-Novakovic, G.** (2004b): Medium perfusion enables engineering of compact and contractile cardiac tissue. *American Journal of Physiology: Heart and Circulatory Physiology*, vol. 286, pp. H507-H516.

**Reinlib, L., and Field, L.** (2000): Cell transplantation as future therapy for cardiovascular disease?: A workshop of the national heart, lung, and blood institute. *Circulation*, vol. 101, pp. e182-e187.

**Ryu, J. H., Kim, I. K., Cho, S. W., Cho, M. C., Hwang, K. K., Piao, H., Piao, S., Lim, S. H., Hong, Y. S., Choi, C. Y., Yoo, K. J., and Kim, B. S.** (2005): Implantation of bone marrow mononuclear cells using injectable fibrin matrix enhances neovascularization in infarcted myocardium. *Biomaterials*, vol. 26, no. 3, pp. 319-326.

**Shimizu, T., Yamato, M., Isoi, Y., Akutsu, T., Setomaru, T., Abe, K., Kikuchi, A., Umezu, M., and Okano, T.** (2002): Fabrication of pulsatile cardiac tissue grafts using a novel 3- dimensional cell sheet manipulation technique and temperature- responsive cell culture surfaces. *Circulation Research*, vol. 90, no. 3, pp. e40-e48.

**Soonpaa, M. H., and Field, L. J.** (1998): Survey of studies examining mammalian cardiomyocyte DNA synthesis. *Circulation Research*, vol. 83, no. 1, pp. 15-26.

**Starling, R. C., and Jessup, M.** (2004): Worldwide clinical experience with the corcap cardiac support device. *J Card Fail*, vol. 10, no. 6 Suppl, pp. S225-233.

**Stathopoulos, N. A., and Hellums, J. D.** (1985): Shear stress effects on human embryonic kidney cells *in vitro*. *Biotechnology and Bioengineering*, vol. 27, pp. 1021-1026.

**Tao, X., Gregory, C., Molnar, P., and Boland, T.** (2004): Fabricating neural and cardiomyogenic stem cell structures by a novel rapid prototyping - the inkjet printing method *MRS Proceedings*.

**Wang, Y., Ameer, G. A., Sheppard, B. J., and Langer, R.** (2002): A tough biodegradable elastomer. *Nature Biotechnology*, vol. 20, pp. 602-606.

**Yamada, T., Yang, J. J., Ricchiuti, N. V., and Seraydarian, M. W.** (1985): Oxygen consumption of mammalian myocardial-cells in culture - measurements in beating cells attached to the substrate of the culture dish. *Analytical Biochemistry*, vol. 145, no. 2, pp. 302-307.

**Yost, M. J., Baicu, C. F., Stonerock, C. E., Goodwin, R. L., Price, R. L., Davis, J. M., Evans, H., Watson, P. D., Gore, C. M., Sweet, J., Creech, L., Zile, M. R., and Terracio, L.** (2004): A novel tubular scaffold for cardiovascular tissue engineering. *Tissue Eng*, vol. 10, no. 1-2, pp. 273-284.

**Zimmermann, W. H., Didie, M., Wasmeier, G. H., Nixdorff, U., Hess, A., Melnychenko, I., Boy, O., Neuhuber, W. L., Weyand, M., and Eschenhagen, T.** (2002a): Cardiac grafting of engineered heart tissue in syngenic rats. *Circulation*, vol. 106, no. 12 Suppl 1, pp. I151-I157.

**Zimmermann, W. H., Fink, C., Kralish, D., Remmers, U., Weil, J., and Eschenhagen, T.** (2000): Three-dimensional engineered heart tissue from neonatal rat cardiac myocytes. *Biotechnology and Bioengineering*, vol. 68, pp. 106-114.

**Zimmermann, W. H., Schneiderbanger, K., Schubert, P., Didie, M., Munzel, F., Heubach, J. F., Kostin, S., Nehuber, W. L., and Eschenhagen, T.** (2002b): Tissue engineering of a differentiated cardiac muscle construct. *Circulation Research*, vol. 90, no. 2, pp. 223-230.

**Zong, X., Bien, H., Chung, C. Y., Yin, L., Fang, D., Hsiao, B. S., Chu, B., and Entcheva, E.** (2005): Electrospun fine-textured scaffolds for heart tissue constructs. *Biomaterials*, vol. 26, no. 26, pp. 5330-5338.